

Mechanical, Tensile Creep and Viscoelastic Properties of Thermoplastic Polyurethane/Polycarbonate Blends

Alper Kasgoz*

Department of Polymer Materials Engineering, Faculty of Engineering, Yalova University, Yalova 77200, Turkey
(Received January 30, 2020; Revised May 11, 2020; Accepted May 16, 2020)

Abstract: This study investigated the morphological, mechanical and solid-state creep properties of thermoplastic polyurethane/polycarbonate blends. Blend film samples were prepared via the solution-mixing method. The morphological and mechanical properties of the samples were investigated by scanning electron microscope (SEM) and universal test machine. Solid-state creep tests were also performed by dynamic mechanic analyzer (DMA) under a stress value of 3 MPa at different temperatures (30, 40, and 50 °C). Morphological observations indicated that the blend samples had a compatible structure due to the polar nature of PC and TPU. In the mechanical tests, it was found that the tensile modulus value improved significantly by incorporation of PC, whereas the strain at break and toughness values reduced. Accordingly, the blend sample that contained PC at the rate of 10 % (wt.) showed a higher tensile modulus and lower toughness than neat TPU by 2.85 and 0.56 times, respectively. In the creep strain analyses, the viscoelastic structure and long-term creep performance of the samples were analyzed by the Burger model, time-temperature superposition (TTS) approach and Findley model. The experimental values and the model predictions indicated that incorporation of PC into the TPU phase improved the creep resistance of TPU significantly. For example, the creep strain value of neat TPU could be reduced by 68 % and 98 % in the respective cases of the PC concentrations of 10 % (wt.) and 50 % (wt.). Finally, the experimental creep-recovery behavior of the samples was investigated, and the permanent strain values were determined by the Weibull Distribution Function (WDF).

Keywords: Thermoplastic polyurethane (TPU), Polycarbonate (PC), Creep properties, Polymer blends

Introduction

Thermoplastic polyurethanes (TPUs), which have a multi-block copolymer structure, are known as the first homogeneous elastomeric materials that can be processed by melt processing methods [1]. TPUs are synthesized from (polyether or polyester based) polyols and polyisocyanate (or diisocyanate) by a condensation reaction, and each component and their different derivatives provide different, unique properties. For instance, hard segments (diisocyanates and the short-chain diols) determine the hardness, tensile modulus, tear resistivity, impact strength and upper use temperature, whereas soft segments determine the flexibility, strain at break and other low-temperature properties [1].

TPUs exhibit many unique properties such as processability by melt processing equipment, adjustable mechanical strength, hardness and modulus values, superior tear and abrasion resistance and high strain at break values. However, they also show weaknesses in some physical properties such as relatively low modulus of elasticity, thermal resistance and creep resistance in comparison to engineering plastics and chemically cross-linked systems. Reinforcement of TPUs has been investigated in many studies to improve their performance for various implementations. In these implementations, there are two main widely used approaches, which change the molecular structure of polyurethane by modifying its monomers [2,3] and introducing an organic/inorganic filler or a second polymer phase [4-8] into the

polyurethane matrix. However, preparation of composites with various organic/inorganic fillers is more commonly preferred due to its advantages such as easiness of processing and low costs.

In one of these studies, Jia *et al.* prepared ozone-treated multi-walled carbon nanotubes filled with TPU and investigated some mechanical properties (such as Young's modulus and yield strength) and creep resistance of the composite samples [9]. In their paper, it was reported that the Young's modulus (16.02 %), tensile strength (10.9 %) and strain at break (14.6 %) values were improved by incorporation of 3 % of ozone-treated multi-walled carbon nanotubes. It was also reported that the creep resistance of TPU was also improved so that the creep strain of neat TPU under the conditions of 35 °C and 5 MPa was reduced by about 70 % by addition of 3 % of ozone-treated multi-walled carbon nanotubes. In another relevant study, Yuan *et al.* prepared TPU nanocomposites filled with carbon nanotubes (CNT) and graphene nanoplatelets (GNP) via melt blending [10]. In their study, it was reported that the GNP- or CNT-filled nanocomposites (filler concentration was 0.1 % by weight) exhibited a higher tensile modulus by 12 % and 19 %, respectively, in comparison to the neat TPU. Creep experiments that were carried out under 1.5 MPa and 100 °C for 10 min indicated that incorporation of the GNP and CNT by 0.1 % reduced the creep strain of neat TPU by ~10 % and ~18 %, respectively. Moreover, it was reported that synergistic effects were also observed in case of especially combining GNP and CNT at a ratio of 6:4, and these hybrid composites exhibited a higher tensile modulus by 22 % and lower creep

*Corresponding author: akasgoz@yalova.edu.tr

strain by ~23 % in comparison to neat TPU.

In this paper, unlike the conventional studies in the literature with aims to improve the creep resistance of TPU by incorporation of inorganic fillers, TPU was blended with PC, which has a higher glass transition temperature and compatibility with TPU than inorganic fillers due to its chemical structure. To the best of the author's knowledge, a comprehensive study has not been reported about improvement of creep resistance of TPU by blending with PC or other rigid amorphous polymers.

Experimental

Material and Preparation of the Blends

Polyester-based TPU (Desmopan 3380A, $d: 1.16 \text{ g cm}^{-3}$) was kindly donated by Bayer (Turkey). Polycarbonate was also kindly provided by DOW Chemicals (DOW Calibre 303EP, melt index: 22 g/10 min, density: 1.2 g/cm^3). Analytical-grade tetrahydrofuran (THF; Sigma-Aldrich, 87368) was used to dissolve the TPU and PC granules. The TPU and PC were dried at 80 °C in a vacuum oven overnight before processing. The blend samples were prepared by the solution casting method. In the method, a proper amount of TPU and PC were dispersed in 50 ml of THF and vigorously stirred by a magnetic stirrer for six hours. Then, the mixture was poured into glass dishes and left at room temperature for 24 h. Finally, the film samples that were obtained were left in a vacuum oven at 80 °C for 48 h for solvent evaporation. Sample compositions and notations are shown in Table 1.

Scanning Electron Microscope (SEM)

The morphological properties of the blend samples were investigated by a scanning electron microscope (FE-SEM, FEI Quanta FEG 450) operated at 30 kV. The cryo-fractured surfaces of the film samples were directly imaged by SEM after proper sample preparation of sputter-coating with gold.

Mechanical Properties

Mechanical properties of the samples were performed by a universal test machine (Zwick/Roell Z020) according to the ASTM-D-882 standard. For each sample, at least four

specimens were tested to provide reproducibility, and the average values are reported.

Creep and Recovery Tests

Uniaxial tensile creep tests of the composite films were performed in a dynamic mechanic analyzer (DMA, ExStar 6100, SII Nanotechnology) under a stress value of 3 MPa at different temperatures (30, 40, and 50 °C). The applied stress value was determined from the stress-strain plot of the samples to be within the linear deformation area for all samples. The width and length of the test specimens were 20 mm and 10 mm, respectively. The creep and recovery periods were applied as 30 min and 15 min, respectively. The test specimens were thermally conditioned at the test temperature for 10 min. before the creep tests.

Results and Discussion

Morphological Properties

The mechanical properties of polymer blends are strongly dependent on their morphological properties such as miscibility, phase structure, adhesion and surface tension of the components. Therefore, controlling the morphology in polymer blends is of great importance. In this concept, before the discussion about mechanical and tensile creep behavior, morphological observations are given in detail. To investigate the variation of the morphology with composition, SEM was used and the obtained micrographs are given in Figure 1(a-f).

In Figure 1(a-d), it may be clearly seen that the spherical particles of PC dispersed homogeneously in the TPU matrix, and these spherical particles were denser with increasing PC content. However, Figure 1(e-f) shows that the morphology of the PC particles approached a fibrillar structure at 50 % of PC content by weight. Despite the equal weight percentages of the TPU and PC, it may also be noted that PC could not form a continuous phase by the coalescence of the droplets or fibrillar PC particles for the sample of TPU50-PC50 due to the lower relative viscosity of PC.

On a microscopic scale, good adhesion between PC and TPU phases may be observed clearly in Figure 1. A possible explanation for this may be the highly polar structure of isocyanate groups and increasing interfacial adhesion due to the presence of hydrogen bonds between PC and TPU. In a relevant study, Li *et al.* prepared blends of TPU and PA1212 that had similar properties to a TPU/PC blend and investigated their mechanical, thermal and morphological properties [11]. In the morphological observation section of their study, they carried out EDAX analyses on the blend samples and revealed that the soft segments of TPU were also aggregated at the interphase. In this respect, the good compatibility of PC and TPU may be attributed to not only the highly polar structure of the rigid isocyanate segment but also the polyol segment.

Table 1. Sample code and contents

Sample	% wt	
	TPU	PC
TPU50-PC50	50	50
TPU60-PC40	60	40
TPU70-PC30	70	30
TPU80-PC20	80	20
TPU90-PC10	80	20
TPU100-PC0	100	0

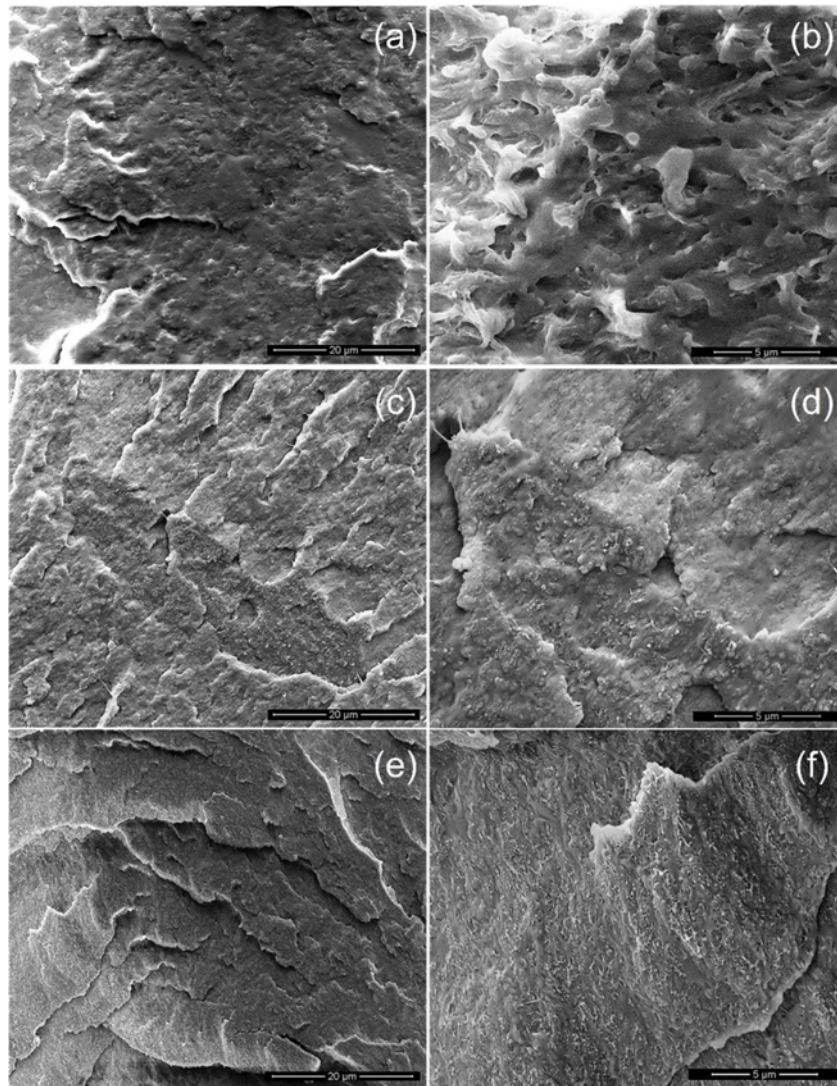


Figure 1. SEM micrographs of the samples (a, b) TPU80-PC20, (c, d) TPU60-PC40, and (e, f) TPU50-PC50.

Mechanical Properties

The tensile stress-strain (S-S) curves of the neat TPU and the blends are given in Figure 2. It is clearly seen that TPU showed a soft elastomeric behavior and elongated by up to 1200 %. Addition of PC to the TPU phase caused progressive changing of the S-S curve characteristics, such that the blend samples containing PC between 10-40 % showed a ductile behavior, and the sample of TPU50-PC50 that contained PC at a rate of 50 % showed a brittle character.

Furthermore, it is seen that TPU did not show a yield, whereas the blend samples exhibited necking between 1-4 % of strain, which may be seen in Figure 2. The evaluated mechanical properties (modulus of elasticity, strain at break, ultimate strength and toughness) of the TPU/PC blends as a function of PC content are summarized in Figure 3(a-d). In Figure 3(a), it is seen that the tensile modulus of TPU with

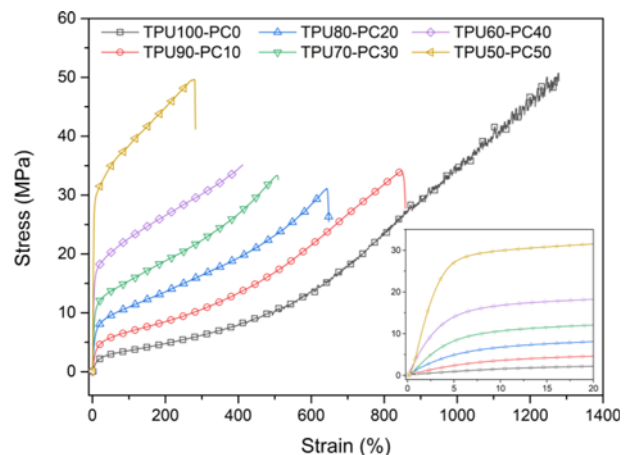


Figure 2. Stress-strain (SS) curve of the samples.

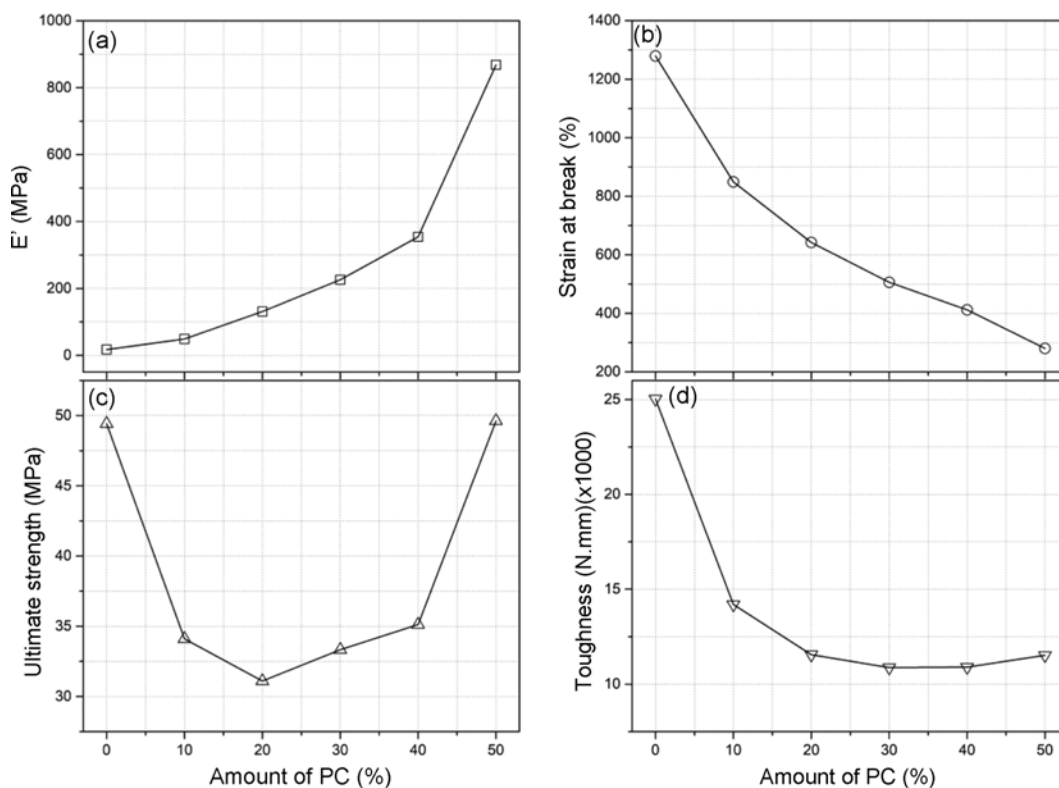


Figure 3. Variation of (a) tensile modulus, (b) strain at break, (c) ultimate strength and (d) toughness of the samples with sample composition.

increasing content of PC was improved due to good compatibility between the phases and the high elastic modulus of PC. As the increasing trend of the E' values of the blend samples were investigated, there was a linear relationship between tensile modulus and percentage of PC for the 10-40% polycarbonate content; however, a significant increase was observed at a polycarbonate content of 50%. In general, it may be assumed that PC acted as a solid particle in the blend due to the very high glass transition temperature ($\sim 150^\circ\text{C}$) [12]. Additionally, it is known that particles with a fibrillar structure and higher aspect ratio (i.e., carbon fiber) are more effective than spherical particles (i.e., carbon black) in enhancement of modulus of elasticity [13]. So, this non-linear increase was attributed to changes in the spherical droplet form of the PC particles into a fibrillar structure at the 50% PC content, which were also revealed by SEM analyses.

The strain at break values of the neat TPU and the blend samples are given in Figure 3(b). In general, the strain at break values may be some of the most critical mechanical parameters to evaluate adhesion between the polymer components of the blend. This is because, in the case that increased the elongation of a polymer blend, tears are expected to start from the interfaces where the strength is expected to be lower. Moreover, in comparison to neat TPU,

the TPU phase of the blends exposed a higher amount of elongation to reach the same strain value, because PC does not show a considerable elongation due to its high mechanical strength. It also caused a higher permanent strain rate in the TPU component of the blends and agglomeration of the applied stress on the polymer interfaces, which cause ruptures at lower elongation rates. In this regard, it is an expected result that the strain at break values decreased with increasing PC content. It should also be noted that the strain at break values of the blend samples decreased more effectively between the PC contents of 40 and 50%. This may also be attributed to changes in the spherical droplet form of the PC particles into a fibrillar structure at this composition, which enables a higher area of the interfaces.

Tensile strength is defined as the maximum capacity of a material to withstand loads tending to elongate, and it is determined as the stress value corresponding to the strain at break from SS curves (Figure 2). The tensile strength values of the samples are presented in Figure 3(c). The Figure shows that the tensile strength of the samples decreased up to a 20% PC content, whereas it started to increase and showed a significant increase between the PC contents of 40 and 50%, such that the sample of TPU50-PC50 had a higher tensile strength value than neat TPU. Changes in the decreasing trend after the 20% PC content could be

probably explained by increases in compatibility of the components and higher interaction of the PC particles, which hindered the viscous chain movement that occurred at the breakpoint. Furthermore, the significant increase at 40-50 % PC may be explained by formation of fibrillar structure of PC particles at this composition.

Toughness values that are defined as the ability of a material to absorb energy up to break are given in Figure 3(d) for all samples. Toughness, which is given as the area under the stress-strain curve, primarily depends on the strain at break and ultimate stress values. Figure 2 shows that the strain at break values were more effective on toughness because the strain values of the samples were much higher than values ultimate stress. As a result, the toughness values of the TPU decreased with incorporation of PC into the TPU phase by up to a PC concentration of 40 % (wt.). However, it should be noted that it started to increase at the higher PC content of 40 %, which may be explained by a significant increase in the ultimate stress values in this range.

Tensile Creep Properties

Creep is defined as the time-dependent deformation of a material under constant stress and temperature [14] and determination of the creep of materials are of great importance, especially for materials that are exposed to a force throughout their lifetimes such as many types of rubbers that are used in production conveyor belt applications, and composites that are used as load-bearing columns in the automobile industry. A typical creep and recovery curve for a viscoelastic material is shown in Figure 4. In Figure 4, it is seen that the first response of the material was an elastic/instantaneous strain (ϵ_{ins}). Then, an elastic-dominant viscoelastic deformation, which is called the primary creep region (ϵ_1), is seen [15,16]. Finally, the viscous character of the specimen becomes more pronounced, and a viscous-dominant

viscoelastic deformation (ϵ_2) is seen, which is called the secondary creep region. The total strain within a particular time is the sum of these strains, called the viscoelastic strain ($\epsilon_v = \epsilon_{ins} + \epsilon_1 + \epsilon_2$) [15,16]. When the stress is removed, the viscoelastic material recovers the elastic strain instantaneously and a part of viscoelastic strain slowly. However, a certain amount of strain cannot be recovered due to viscous deformation during the creep stage, and it is called permanent strain. If the loading stress is close to the yield point, and/or tests are performed at relatively higher

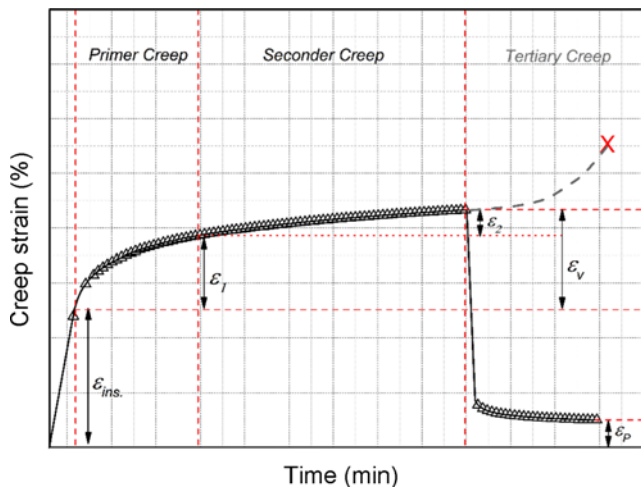


Figure 4. Creep and relaxation characteristics of a viscoelastic material.

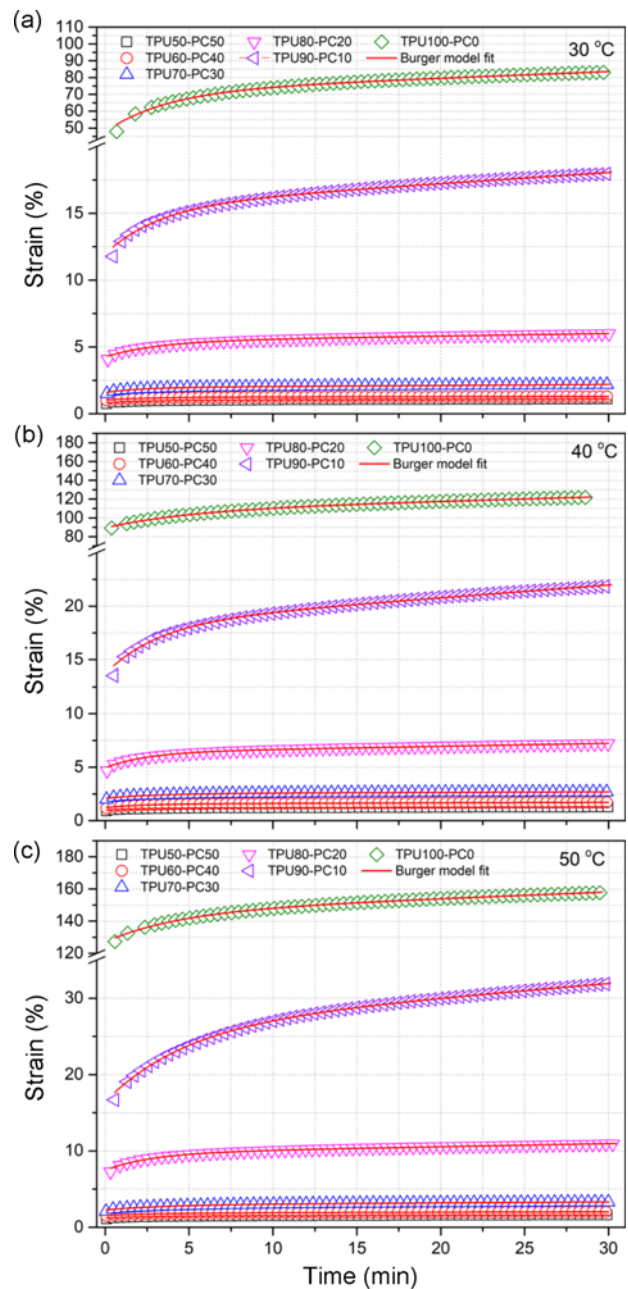


Figure 5. Variations in creep strain of the samples for (a) 30 °C, (b) 40 °C, and (c) 50 °C test temperatures.

Table 2. Reduction in creep strain of TPU

Sample code	Temperature (°C)		
	30	40	50
TPU100-PC0	-	-	-
TPU90-PC10	64.08 %	81.96 %	79.81 %
TPU80-PC20	92.8 %	94.1 %	93.09 %
TPU70-PC30	97.4 %	97.8 %	97.9 %
TPU60-PC40	98.44 %	98.6 %	98.7 %
TPU50-PC50	98.67 %	98.95 %	98.97 %

temperatures and/or within a relatively longer time, the sample might experience an increasing creep rate which could cause rupturing or breaking known as *tertiary creep* [9,11].

Figure 5(a-c) displays the creep strain of the samples for different test temperatures as a function of time. In the Figure, it is clearly seen that all samples showed instantaneous deformation, primary and secondary creeps, whereas there was no evidence of tertiary creep or creep rupture, which would require longer test times or higher stress levels.

The results that are shown in Figure 5 also indicated that the creep strain of the blends was much lower than that of neat TPU for all test temperatures, and this implied that decreases in the creep strain of the blends were more pronounced with PC content.

To reveal the effect of PC concentration and test temperature on the reduction in creep strain of the blends for all test temperatures, the relative decrease in the creep strain of TPU by addition of PC is shown in Table 2 for each test temperature. The relative decrease values in creep values were obtained by dividing the strain values of the blend samples by strain value of TPU for the same temperature. Table 2 shows that the strain value of neat TPU at 30 °C was reduced by 64.08 % and 98.67 % when the PC concentration was respectively 10 % (wt.) and 50 % (wt.). However, in the case that the test temperature was 50°C, the relative decrease values were determined as 79.81 % (wt.) and ~99 % (wt.) for PC concentrations of 10 % (wt.) and 50 % (wt.), respectively. When the changes in creep strain were evaluated based on the blend composition, reduction of the creep strain of the blends with increasing PC concentration could be attributed to hindering of the chain movements of TPU by PC that acted as a solid phase or particles in test temperatures due to the very high glass transition temperature. In addition, considering the relative decreases in the strain values given in the table, it was also noted that that the relative decrease in the creep strain of TPU90-PC10 increased with temperature, however this temperature dependency disappeared with increasing PC content. The comparison of the experimental results that were obtained to those in the literature indicated that PC may be used effectively to reinforce the creep resistance and tensile

modulus of TPU [4-8]. This significant reinforcement effect of PC could be attributed to the solid behavior of the PC at the test temperatures and higher interaction/compatibility between the TPU and PC, which enabled a better homogenous dispersion of PC particles and less slipping movements at the interfaces of the TPU and PC phases.

Modelling of Creep Behavior

In general, modeling of the creep behavior of polymeric materials is performed for two purposes, which are illuminating the viscoelastic structure and prediction of the long-term performance. Modelling about the viscoelastic structure may provide much comprehensive information such as structure-property relationships, the portion of elastic and viscous deformation in total deformation and the relaxation coefficient. In the literature, many two-, three- or four-element viscoelastic models have been developed and used to define the relationship between viscoelastic structure and material characteristics [17,18]. In these models, spring and dashpot, which typically characterize elastic and viscous behaviors, were simply combined in various configurations. One of the most commonly used models is the four-element Burger model [16,19,20], which is a simple combination of the Maxwell and Kelvin-Voigt models. The schematic representation of the Burger model is shown in Figure 6.

Under the condition of linear deformation, the total strain of a viscoelastic solid may be given as the sum of immediate elastic deformation of Maxwell spring (ε_{M1}), delayed elastic deformation of Maxwell dashpot (ε_{M2}) and viscous deformation of Kelvin unit (ε_K) (equation (1)).

$$\varepsilon(t) = \varepsilon_{M1} + \varepsilon_K + \varepsilon_{M2} \quad (1)$$

Considering the combination of the Maxwell and Kelvin-Voigt elements in the Burger model, the mathematical representation of the Burger model may be given as follows;

$$\varepsilon(t) = \frac{\sigma}{E_M} + \frac{\sigma}{E_K} \left[1 - \exp\left(-\frac{E_K t}{\eta_K}\right) \right] + \frac{\sigma t}{\eta_M} \quad (2)$$

where E_M and η_M are the modulus and viscosity of the Maxwell spring and dashpot, respectively; E_K and η_K are the

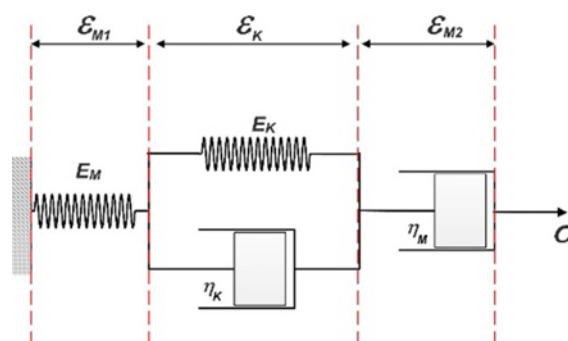
**Figure 6.** Schematic representation of Burger viscoelastic model.

Table 3. Burger Model parameters for the samples at different temperatures

Sample code	30 °C				40 °C				50 °C			
	E_m (MPa)	E_k (MPa)	η_m (MPa·min)	η_k (MPa·min)	E_m (MPa)	E_k (MPa)	η_m (MPa·min)	η_k (MPa·min)	E_m (MPa)	E_k (MPa)	η_m (MPa·min)	η_k (MPa·min)
TPU50-PC50	3.68	14.9	936.6	0.45	3.08	15.9	739.5	29.2	2.5	11.2	537.9	31.3
TPU60-PC40	2.87	14.9	1698.3	7.99	2.46	8.9	564.9	19.1	1.9	9.9	557.4	32.3
TPU70-PC30	1.88	8.08	400.6	17.9	1.43	6.9	567.2	21.5	1.32	4.4	240.2	16.5
TPU80-PC20	0.71	2.57	152.8	43.4	0.61	2.1	106.1	5.1	0.4	1.3	73.4	3.78
TPU90-PC10	0.25	0.83	36.19	2.70	0.22	0.63	25.15	2.1	0.18	0.30	16.45	1.44
TPU100-PC00	0.063	0.12	7.64	35.7	0.03	0.16	7.52	0.8	0.02	0.16	7.3	0.72

modulus and viscosity of the Kelvin spring and dashpot, respectively, and σ is the applied stress value. The experimental creep data of the samples were fitted with the Burger equation by employing a non-linear curve-fitting function in the OriginPro 9.0 software. The fitting results are given in Figure 5 with a red line for each sample, and the calculated Burger parameters are listed in Table 3. It may be clearly seen in Figure 5 that the Burger equation successfully fit the experimental data for each condition.

In the model, the parameter E_M is determined from the instantaneous strain section of the creep strain-time plots, in which stress is applied to a sample instantaneously, and this applied stress is compensated by the crystalline or solid content of polymeric materials dominantly. Therefore, the variation in E_M values is strongly attributed to the degree of crystallinity or solid particle content for polymeric materials. Table 3 shows that the E_M values of the samples increased with PC content, whereas they decreased with temperature. Considering both of PC and TPU have amorphous structures, the variation in the E_M values could be related to the solid-like behavior of PC in the test temperature ranges due to its very high T_g value. On the other hand, unlike the variation in the E_M values with temperature, it could be observed that, from the literature about the dynamic mechanical analyses of PC, the modulus of elasticity values of PC ($\log(E')$ -temperature) do not change considerably with temperatures between 30 and 50 °C [12]. In this respect, decreases in the E_M values of the blends with temperature could be attributed to decreasing of E' values of the TPU with increasing temperature and the sliding of solid PC particles on themselves because the amorphous TPU chains have very low T_g and located between the solid PC particles.

E_K and η_K , which are related to the Kelvin unit of the Burger model, define the primary creep region of the materials. In this region, firstly, the highly elastic strain is seen due to the stretching movements of the amorphous TPU chains.

This predominantly elastic strain is represented by the Kelvin spring in the model and associated with the E_K parameter. In the case that the stress that is applied is maintained, viscous deformation of the structure occurs and

starts to be more effective with time due to the sliding of the polymer chains on themselves. The resulting viscous deformation of the samples is represented by the dashpot in the Kelvin unit, and it is associated with the η_K parameter. In Table 3, it is seen that both E_K and η_K increased with PC content of the blend samples, which could be attributed to the hindering of TPU chain movements by solid PC particles.

Finally, another significant parameter about the viscous character of a viscoelastic sample is η_M , which is represented by the Maxwell dashpot element of the Burger Model and related to unrecoverable creep strain. From Table 3, it is seen that addition of PC into the TPU matrix caused an increase in the η_M values, whereas temperature caused a decrease in the η_M values, as expected. To investigate irrecoverable creep deformation of the samples, WDE is also employed in experimental recovery data in the section of *Creep-Recovery*.

In general, as it may be seen in Figure 5, the creep strain of a viscoelastic material increases with time, whereas the strain rate decreases. In this respect, theoretically, it is supposed that the creep rate ($\dot{\epsilon}$) of a viscoelastic material reaches a constant value after a certain period, which is sufficient for stretching the Maxwell spring completely.

Accordingly, a constant creep rate value is related to the Maxwell dashpot element of the Burger model (η_M) and calculated by the second-order derivative of the Burger Model (equation (3)) [18].

$$\dot{\epsilon}(\infty) = \frac{\sigma_0}{\eta_M} \quad (3)$$

The $\dot{\epsilon}$ values of the samples that were calculated are given in Figure 7 for all test temperatures. Figure 7 shows that the constant creep rate of the samples decreased significantly up to a polycarbonate content of 30 %; however, it was almost constant between the PC concentrations of 30 and 50 %. Decreasing of the constant creep values of the blends with increasing PC content could be explained by that PC does not show considerable permanent deformation in test temperatures (30, 40 and 50 °C) and stress (3 MPa) due to its high T_g (149±1 °C) and tensile modulus values [21].

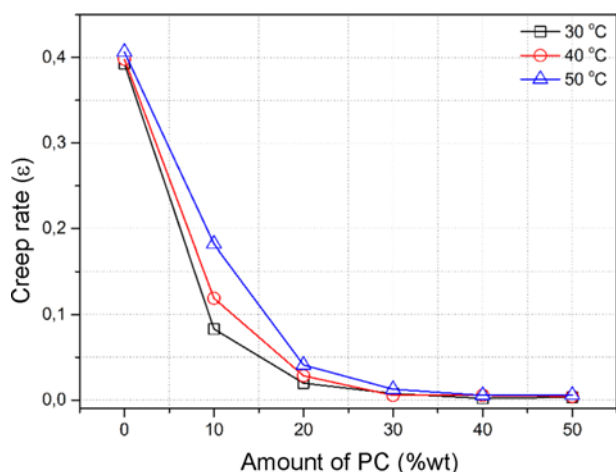


Figure 7. Variation of the theoretical constant creep rates values with sample composition.

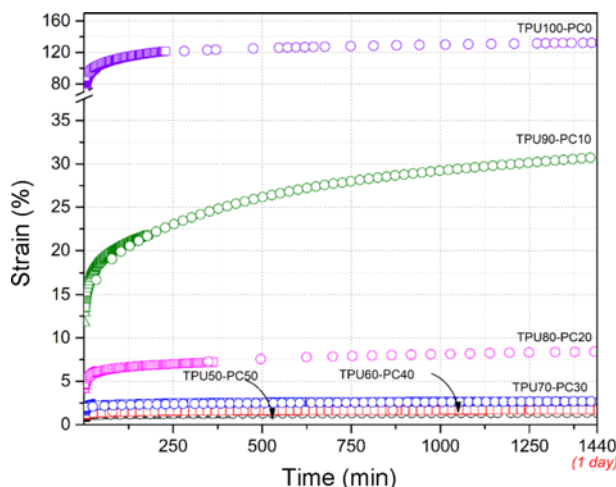


Figure 8. Creep strain prediction of 1-day performance of the samples obtained by TTS approach.

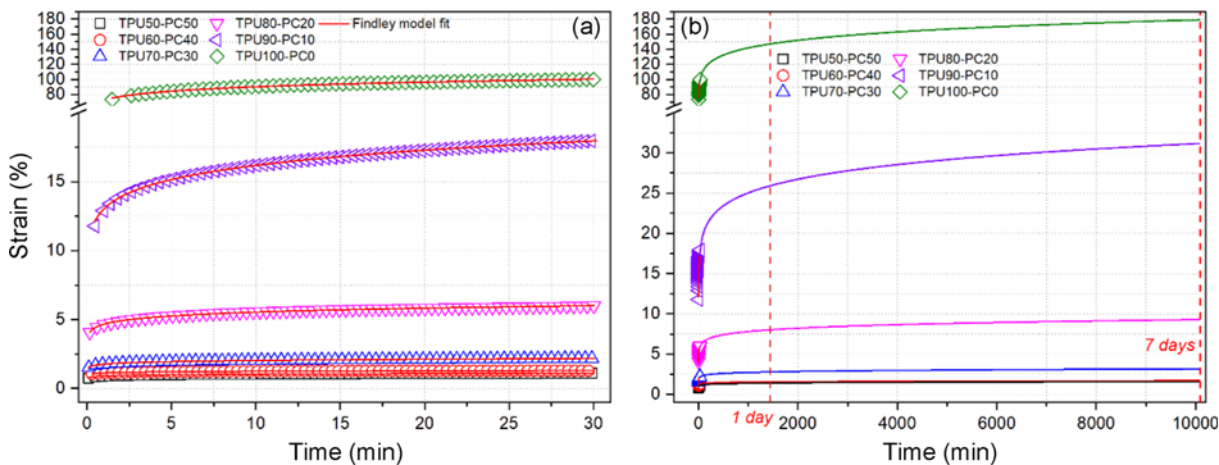


Figure 9. (a) Modeling results of experimental creep strain data obtained at 30 °C and (b) prediction of long-term creep strain values of the samples obtained by simulation of Findley model.

Likewise, good compatibility between the TPU and PC matrix and the hindering chain movements of the TPU phase by the solid PC phase also contributed to decreasing creep rates with increasing PC contents.

Another significant effort about modelling of creep behavior is prediction of the long-term performance or determination of the thermomechanical lifetime of a viscoelastic material. Various approaches have been used in the literature for this purpose, such as the time-temperature superposition (TTS) principle, Findley power-law model and Burger four-parameter model [18]. In this paper, the TTS and Findley models were used due to their higher consistency with experimental values [18]. Applying the TTS model and obtaining long-term creep strain values were explained in reference [22]. The long-term strain predictions of the samples, which were obtained by TTS, are presented in Figure 8 for the reference temperature of 30 °C. From the Figure, it is predicted that neat TPU showed a creep strain value of ~140 %, whereas TPU90-PC10 and TPU50-PC50 showed values of only 29 % and 1 %, respectively, at the end of 24 hours. According to the TTS approach, creep tests have to be carried out up to much higher temperatures to extend the predicted period to one week or one month. However, non-linear deformations will occur in the material structure at higher test temperatures, and the consistency of the model will be lost. Therefore, in this paper, the Findley model was also used to predict the creep deformations that would occur in longer periods.

The Findley is a model that defines the creep characteristics of viscoelastic materials in an power-law equation and allows predicting the long-term behavior of these materials [16,18,20]. The model is represented as;

$$\epsilon_F = \epsilon_{F0} + \epsilon_{F1}t^n \tag{4}$$

where ϵ_F is the total creep strain at time t , ϵ_{F0} is the

Table 4. Findley Model parameters for the samples for 30 °C

Sample code	ε_{F0}	ε_{F1}	n	r^2
TPU50-PC50	0.01	0.8962	0.060	0.995
TPU60-PC40	0.15	0.98	0.049	0.973
TPU70-PC30	0.152	1.617	0.067	0.998
TPU80-PC20	0.158	4.51	0.076	0.998
TPU90-PC10	0.165	12.85	0.096	0.999
TPU100-PC00	9.4	63.28	0.107	0.996

instantaneous initial strain, ε_{F1} is the time-dependent creep strain, and n is the stress-independent time exponent. In the application of the model, the experimental creep values were fitted by the model equation, and then, the related coefficients were determined for each sample. Finally, the specific coefficients obtained for each sample were replaced in the equation, and the time axis was simulated to the desired range. Thus, the long-term creep plot was obtained. Fitting of the Findley model to the experimental creep values for each sample is shown in Figure 9(a) with a red line, and the calculated parameters are listed in Table 4 for the measurement carried out at 30 °C. It is clearly seen that the model successfully fit the experimental data. Figure 9(b) illustrates the long-term strain prediction curves of the samples up to 7 days for the test conditions of 3 MPa and 30 °C. To confirm the reliability of the model, the creep strain values of the samples at the end of 24 hours which were predicted by the TTS and Findley models were compared, and it was clearly seen that similar values were obtained by both methods. From this point of view, simulations covering the longer period were carried out with the Findley model, and the results were evaluated. Figure 9(b) indicates that neat TPU showed a creep strain value of ~180 %, whereas TPU90-PC10 and TPU50-PC50 showed only 31 % and 1.57 %, respectively, at the end of 7 days.

Creep-Recovery Behavior

In the last part of the study, the creep recovery behavior of the samples was examined experimentally and theoretically. Figure 10(a-c) shows the fitting results of the experimental curves of the recovery strain as a function of time. When the permanent strain values at the end of the recovery period were examined, it was clear that addition of PC significantly reduced the permanent strain rates in the blend samples. In the creep tests, the duration of the recovery section was also kept short due to various time limitations. In such cases, WDF is commonly used to predict the recovery ratio and permanent strain. The Weibull equation is known as [23,24];

$$\varepsilon_r(t) = \varepsilon_v \left[\exp\left(-\left(\frac{t-t_0}{\eta_r}\right)^{\beta_r}\right) \right] + \varepsilon_\infty \quad (5)$$

where ε_v is the viscoelastic strain recovery determined by two parameters including the characteristic life (η_r) and

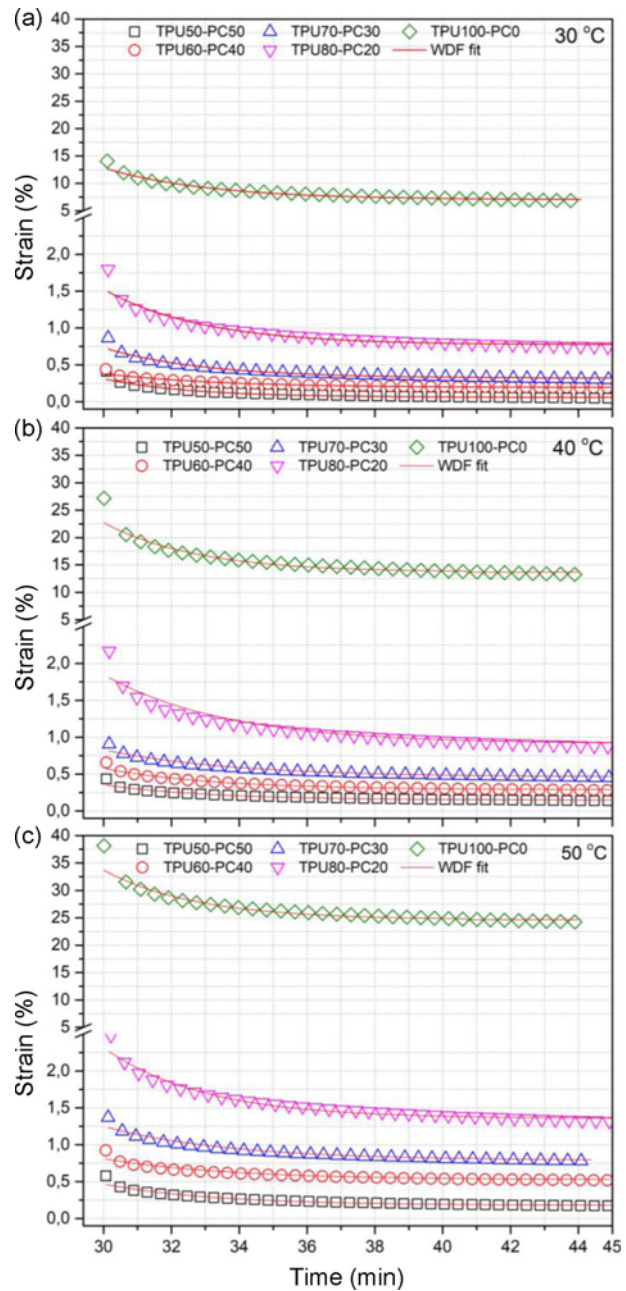


Figure 10. Modeling of relaxation behavior of samples with the WDF; (a) 30 °C, (b) 40 °C, and (c) 50 °C.

shape (β_r) parameters over recovery time t , t_0 is the time when the stress loading is removed, and ε_∞ is the permanent strain due to viscous flow effects. By using the Weibull function, the values of ε_∞ and ε_v are determined, and then, the elastic (instantaneous) deformation which corresponds to the strain of Maxwell spring (ε_E) can be obtained by using the equation (6) [23,24]:

$$\varepsilon_E = \varepsilon_{\max} - \varepsilon_v - \varepsilon_\infty \quad (6)$$

Table 5. Weibull model parameters for the samples at different temperatures

Sample code	Temperature											
	30 °C				40 °C				50 °C			
	ε_v	ε_∞	ε_E	ε_{max}	ε_v	ε_∞	ε_E	ε_{max}	ε_v	ε_∞	ε_E	ε_{max}
TPU50-PC50	0.25	0.06	0.8	1.11	0.21	0.15	0.92	1.28	0.29	0.18	1.16	1.63
TPU60-PC40	0.19	0.19	0.92	1.30	0.29	0.29	1.13	1.71	0.29	0.52	1.21	2.02
TPU70-PC30	0.41	0.32	1.45	2.18	0.37	0.46	1.86	2.69	0.46	0.79	2.06	3.31
TPU80-PC20	0.75	0.77	4.46	5.98	0.94	0.91	5.35	7.20	0.96	1.36	8.59	10.91
TPU90-PC10	1.63	1.55	26.8	29.98	1.83	2.59	17.58	22	3.80	3.03	25.07	31.9
TPU100-PC00	5.80	7.028	70.6	83.46	9.04	13.69	99.27	122	9.04	24.67	124.29	158

where ε_{max} is the maximum deformation measured by the creep tests. The model parameter values are listed in Table 5. In the Table, it is clearly seen that all strain values (ε_v , ε_∞ , ε_E , ε_{max}) decreased with PC content, which was expected due to the inhibition effect of solid PC particles. Based on the parameters obtained from the Burger's equation and the Weibull distribution function, it could be concluded that incorporation of the PC phase into the TPU structure yielded an increase in viscosity (η_M and η_K) and modulus (E_K and E_M), thus, partly restricted the elastic and viscous chain mobility of TPU.

Conclusion

In the study, thermoplastic polyurethane (TPU)/ polycarbonate (PC) blends were prepared, and morphological, mechanical and solid-state tensile creep properties were investigated. In the morphological observation, it was seen that the blend sample containing 20 % of PC by weight (TPU80-PC20) exhibited a ductile fracture. However, the samples containing 40 % and 50 % of PC by weight showed a fragile fracture due to the increasing content of PC that has a glassy behavior at the measurement temperature (Figure 2(c-f)). The stress-strain curves of the samples indicated that addition of PC to the TPU phase caused progressive changes such that TPU showed a soft elastomeric behavior, blend samples containing PC between 10 and 40 % showed a ductile behavior, and the sample of TPU50-PC50 that contained PC at a rate of 50 % showed a brittle character. It was found that the tensile modulus value improved significantly by incorporation of PC, whereas the strain at break and toughness values decreased. Ultimate stress value was also lower than neat TPU at lower PC concentrations (10-40 % by wt.), but the blend sample containing PC by 50 % (wt.) had an approximately similar value to that of TPU. Creep analyses of the samples indicated that the creep strain of the blends was much lower than that of neat TPU at all test temperatures, and this implied that the decrease in the creep strain of the blends were more pronounced with PC content. When the changes in creep strain were evaluated according to the blend composition, reduction in the creep

strain of the blends with increasing PC concentration was attributed to hindering of chain movements of TPU by PC that acted as a solid phase or particles at the test temperatures due to the very high glass transition temperature. Comparison of the experimental results that were obtained to those in many previous studies indicated that PC could be used more effectively than most organic or inorganic fillers for improvement of the creep resistance of TPU, because PC has a higher compatibility with TPU than many inorganic fillers and acts as a solid particle in test conditions due to its T_g value.

References

1. J. G. Drobny, "Handbook of Thermoplastic Elastomers", Elsevier, 2014.
2. A. Eceiza, M. Martin, K. De La Caba, G. Kortaberria, N. Gabilondo, M. Corcuera, and I. Mondragon, *Polym. Eng. Sci.*, **48**, 297 (2008).
3. H. Tanaka and M. Kunimura, *Polym. Eng. Sci.*, **42**, 1333 (2002).
4. D. A. Nguyen, Y. R. Lee, A. V. Raghu, H. M. Jeong, C. M. Shin, and B. K. Kim, *Polym. Int.*, **58**, 412 (2009).
5. J. Fallon, B. Kolb, C. Herwig, E. Foster, and M. Bortner, *J. Appl. Polym. Sci.*, **136**, 46992 (2019).
6. N. Ercan, A. Durmus, and A. Kaşgöz, *J. Thermoplast. Compos. Mater.*, **30**, 950 (2017).
7. G. Kumar, N. Neelakantan, and N. Subramanian, *Polym. -Plast. Technol. Eng.*, **32**, 33 (1993).
8. E. G. Bajsić and V. Rek, *e-Polymers*, **4**, 073 (2004).
9. Y. Jia, Z. Jiang, X. Gong, and Z. Zhang, *Express Polym. Lett.*, **6**, 750 (2012).
10. D. Yuan, D. Pedrazzoli, G. Pircheraghi, and I. Manas-Zloczower, *Polym.-Plast. Technol. Eng.*, **56**, 732 (2017).
11. W. Li, J. Liu, C. Hao, K. Jiang, D. Xu, and D. Wang, *Polym. Eng. Sci.*, **48**, 249 (2008).
12. Y. Sung, C. Kum, H. Lee, N. Byon, H. G. Yoon, and W. N. Kim, *Polymer*, **46**, 5656 (2005).
13. A. Kasgoz, D. Akin, A. I. Ayten, and A. Durmus, *Compos. Part B-Eng.*, **66**, 126 (2014).
14. L. W. McKeen, "The Effect of Creep and other Time

- Related Factors on Plastics and Elastomers”, Elsevier, 2009.
15. A. Kasgoz, M. Tamer, C. Kocyigit, and A. Durmus, *J. Appl. Polym. Sci.*, **135**, 46350 (2018).
 16. Y. Jia, K. Peng, X.-L. Gong, and Z. Zhang, *Int. J. Plast.*, **27**, 1239 (2011).
 17. A. Shokuhfar, A. Zare-Shahabadi, A.-A. Atai, S. Ebrahimi-Nejad, and M. Termeh, *Polym. Test.*, **31**, 345 (2012).
 18. J.-L. Yang, Z. Zhang, A. K. Schlarb, and K. Friedrich, *Polymer*, **47**, 6745 (2006).
 19. I. M. Ward and J. Sweeney, “Mechanical Properties of Solid Polymers”, John Wiley & Sons, 2012.
 20. W. N. Findley and F. A. Davis, “Creep and Relaxation of Nonlinear Viscoelastic Materials”, Courier Corporation, 2013.
 21. V. Yannas and A. C. Lunn, *J. Macromol. Sci. Part B*, **4**, 603 (1970).
 22. A. Kasgoz, D. Akin, and A. Durmus, *Macromol. Mater. Eng.*, **301**, 1402 (2016).
 23. K. S. Fancey, *J. Polym. Eng.*, **21**, 489 (2001).
 24. L. Vas and P. Bakonyi, *Express Polym. Lett.*, **6**, 987 (2012).